Discrete vortex bound states with a van Hove singularity in the vicinity of the Fermi level

Delong Fang(方德龙)[†] and Yunkang Cui(崔云康)

School of Mathematics and Physics, Nanjing Institute of Technology, Nanjing 211167, *China*

(Received 13 September 2022; revised manuscript received 9 November 2022; accepted manuscript online 29 November 2022)

A theoretical study on discrete vortex bound states is carried out near a vortex core in the presence of a van Hove singularity (VHS) near the Fermi level by solving Bogoliubov–de Gennes (BdG) equations. When the VHS lies exactly at the Fermi level and also at the middle of the band, a zero-energy state and other higher-energy states whose energy ratios follow integer numbers emerge. These discrete vortex bound state peaks undergo a splitting behavior when the VHS or Fermi level moves away from the middle of the band. Such splitting behavior will eventually lead to a new arrangement of quantized vortex core states whose energy ratios follow half-odd-integer numbers.

Keywords: vortex bound states, van Hove singularity, Fermi level, density of states

PACS: 74.25.Jb, 74.25.Ha, 74.25.Op **DOI:** 10.1088/1674-1056/aca6d6

1. Introduction

Quantized vortices appear in type-Ⅱ superconductors when the applied magnetic field exceeds the lower critical field. Within a vortex core, cooper pairs are excited into bound states which are confined by the superfluid on the scale of the coherence length ξ. These localized Caroli–de Gennes–Matricon (CdGM) states are predicted to be at energies of $E_\nu = \nu\Delta^2/E_\mathrm{F}$ with ν being the angular momentum quantum number ($\nu = \pm 1/2,\ \pm 3/2,\ \pm 5/2, \ldots$), Δ the superconducting gap and E_F the Fermi energy.[1] Discrete vortex bound states are difficult to be observed in experiments for the very-small level spacing of Δ^2/E_F compared with the spectroscopic energy resolution. In recent years, thanks to the application of low-temperature scanning tunneling microscopy in the quantum limit of $T/T_\mathrm{c} \leq \Delta/E_\mathrm{F}$[2] with T_c the critical temperature, discrete CdGM states were observed in Fe(Se,Te),[3–5] $(Li_{0.84}Fe_{0.16})$OHFeSe,[6,7] the FeSe monolayer,[8] $KCaFe_4As_4$,[9] and $KCa_2Fe_4As_4F_2$.[10] Among these materials, the possible Majorana zero modes were also observed to coexist with the CdGM states,[4–7,9] whose energy ratios follow integer numbers, which are different from those of the conventional CdGM states. Even in the absence of Majorana zero modes, energy ratios of the CdGM states were reported to deviate from the ideal value 1:3:5.[11]

Vortex bound states may reflect band-structure effects.[12] Especially, the anisotropic Fermi surface will concentrate more low-energy quasiparticles traveling along directions of curvature minima.[13,14] The characteristic of saddle points is another crucial information for an electronic band. A two-dimensional saddle point in the electronic dispersion causes a logarithmic or power-law divergence in the density of states (DOS) called van Hove singularity.[15] Theoretically, a VHS in the vicinity of the Fermi level can play an important role in controlling the interplay among superconductivity, spin-density wave, charge-density wave, and in inducing exotic chiral superconductivity.[16–21] Experimentally, the VHS near the Fermi level has been found in a variety of superconductors.[22–24]

In this paper, the large-scale BdG calculation of discrete vortex core states is presented by considering one-band structures with van Hove singularities in the vicinity of the Fermi level. We find that the arrangement of quantized bound states can be dramatically changed by the VHS near the Fermi level. A zero-energy and other integer quantized states can be induced when the VHS and Fermi level are both exactly at the middle of the band. A peak-splitting behavior links this integer quantization and the conventional half-odd-integer quantization of vortex bound states.

2. Model

The superconducting state is described with the following mean-field Hamiltonian:

$$H = \sum_{ij} \Psi_i^\dagger \begin{pmatrix} -t_{ij} - \mu\delta_{ij} & \Delta_{ij} \\ \Delta_{ij}^* & t_{ij} + \mu\delta_{ij} \end{pmatrix} \Psi_j. \tag{1}$$

Here, $\Psi_i = (c_{i\uparrow}, c_{i\downarrow}^\dagger)^\mathrm{T}$ is a real-space Nambu spinor, and the operators $c_{i\sigma}$ ($c_{i\sigma}^\dagger$) annihilate (create) electrons with spin σ at lattice site i. The hopping matrix t_{ij} and chemical potential μ describe the band structure and Fermi level. Our square-lattice tight-binding model includes nearest-neighbor (t_1) and next-nearest-neighbor (t_2) hoppings. Therefore, the dispersion relation is given by $\varepsilon(k) = -2t_1(\cos k_x + \cos k_y) - 4t_2 \cos k_x \cos k_y - \mu$ with $t_1 > 0$ ($t_2 < 0$). For the simplest situation with $t_2 = \mu = 0$, the band structure along two perpen-

[†]Corresponding author. E-mail: fangdel@njit.edu.cn

© 2023 Chinese Physical Society and IOP Publishing Ltd

dicular directions crossing at $(\pi,0)$ is shown in Fig. 1(a). It is obvious that there exist saddle points at the M points. The corresponding DOS of normal state in Fig. 1(c) shows a VHS exactly at the Fermi level. In addition, the VHS is in the middle of the band, i.e., $E_v/W = 0.5$, where E_v is the energy of the VHS from the band bottom and W is the bandwidth of $8t_1$. By tuning t_2 with respect to t_1, the VHS approaches either to the bottom or to the top of the band. If μ is fixed to $4t_2$, the VHS will always be at the Fermi level. Figures 1(b) and 1(d) show the band structure and normal state DOS for another model with $t_2 = -0.2t_1$ and $\mu = 4t_2$. The VHS is located at $0.3W$ from the band bottom.

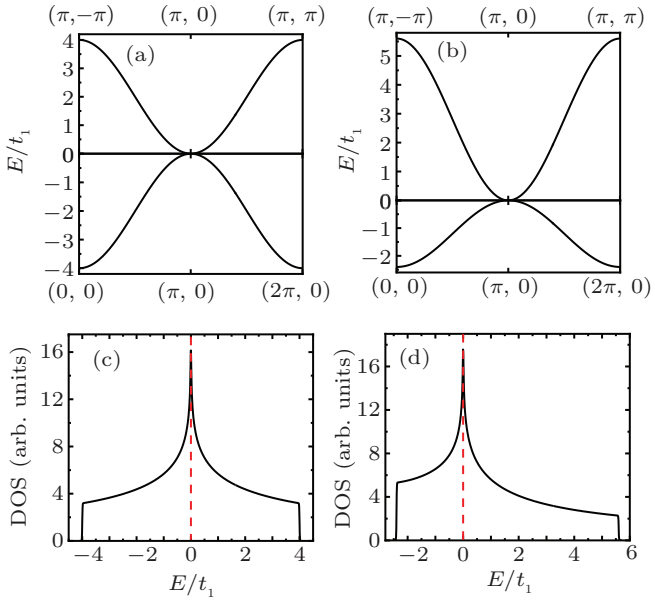


Fig. 1. Band structures [(a), (b)] and the corresponding DOS of normal states [(c), (d)] for two models. The band dispersions are plotted along two perpendicular high-symmetry directions centered at an M point in the Brillouin zone. The dashed red lines in (c) and (d) show that both VHSs are lying exactly at Fermi levels. For these two band structures, the VHSs are located at the middle of the band [(a), (c)] and at $0.3W$ [(b), (d)], respectively, with W being the bandwidth.

The Δ_{ij} is the pairing potential. In this paper, only the on-site pairing is considered. We deal with the Hamiltonian by the non-self-consistent calculation. An isolated vortex in the center of a 601×601 square lattice is imposed to be the form of

$$\Delta_{ii} = \Delta_0 \tanh(r_i/\xi)\, \mathrm{e}^{\mathrm{i}\varphi_i}, \tag{2}$$

where r_i is the radial distance of site i, and φ_i is its azimuthal angle. The coherence length ξ and Δ_0 are set to $18a$ and $0.05t_1$, respectively, where a is the lattice constant.

We diagonalize the Hamiltonian of Eq. (1) by using the real-space recursion method.[25–27] For example, in order to calculate the DOS at site i, we start from $c^{\dagger}_{i\uparrow}|0\rangle$, where $|0\rangle$ is the vacuum, as an initial state, and apply the standard Lanczos method to get a tridiagonal matrix on the $K+1$-dimensional Krylov space of H with $\{a_k; k = 0, \ldots, K\}$ and $\{b_k; k = 1, \ldots, K\}$ as diagonal and subdiagonal elements, respectively. Then, the retarded local Green's function at site i can be written in the form of a continued fraction

$$G(i,\omega) = \cfrac{1}{\omega + \mathrm{i}\eta - a_0 - \cfrac{b_1^2}{\omega + \mathrm{i}\eta - a_1 - \cfrac{b_2^2}{\cdots}}}, \tag{3}$$

where η is a smearing factor, which is chosen as a quite small value of $0.00001t_1$ to enhance the energy resolution. Finally the DOS is obtained as

$$N(i,\omega) = -\frac{1}{\pi}\mathrm{Im}\, G(i,\omega). \tag{4}$$

3. Results and discussion

The DOS near vortex cores for the above two band structures in Fig. 1 are shown in Figs. 2(a) and 2(b), respectively. With a quite small smear factor, sharp and discrete bound state peaks can be clearly seen. When the Fermi level and VHS are both located at the middle of the band, a zero-energy bound state peak emerges as shown in Fig. 2(a). At the vortex core, higher-energy peaks are suppressed by the high-intensity zero-energy peak. When moving slightly away from the vortex core, more periodic bound state peaks emerge with a level spacing δ_1 of about $0.00147t_1$. Ratios of these bound state energies follow integer numbers, which differ from those of the conventional CdGM states calculated before. Such a half-integer level shift also exists in possible topological superconductors which host Majorana zero modes.[4–7,9] For all sites, the DOSs are particle-hole symmetric, probably due to the particle-hole symmetric normal state DOS. When the VHS and Fermi level shift away from the middle of the band, the DOSs near a vortex core change dramatically as shown in Fig. 2(b). After the energy of the horizontal axis normalized by δ_2 of about $0.00151t_1$, it seems that each peak in Fig. 2(a) splits into two subpeaks with a level spacing of about $0.00035t_1$. The zero-energy peak is also replaced by two symmetric subpeaks in energy whose intensity is much higher at the positive energy than that at the negative energy. This particle-hole asymmetry is explained as the quantum limit behavior[2] whose higher DOS peak is at energy $\Delta_2/2E_F$ above (below) the Fermi energy for an electron (hole) band. In our calculations, the higher DOS peak is at positive (negative) energy if the VHS (exactly at the Fermi level) is closer to the band bottom (top).

Figure 3 shows the splitting behavior more clearly. The spatial evolutions of the DOS for a series of bands with VHSs and Fermi levels located at $0.1W$, $0.2W$, $0.3W$, $0.4W$, and $0.5W$ are presented. For each figure, the spectra at vortex core and five nearest sites along the $\theta = 0°$ direction are shown, and the energy of the horizontal axis is normalized by the average

level spacing δ_i. From each figure, we can see the highest peak shifts farther away from the vicinity of the Fermi level with increasing distance from the vortex center, and the intensity of peaks for a selected energy has a oscillatory behavior implying the Friedel oscillation.[10] When the VHS and Fermi level move from the middle to the bottom of the band ($E_v/W = 0.5$ to 0.1), the level spacing of each pair of subpeaks becomes larger and eventually close to the value of $\delta_i/2$. When the VHS and Fermi level are quite far away from the band middle ($E_v/W = 0.1$), all the subpeaks are rearranged as half-odd-integer quantization like the traditional CdGM states.

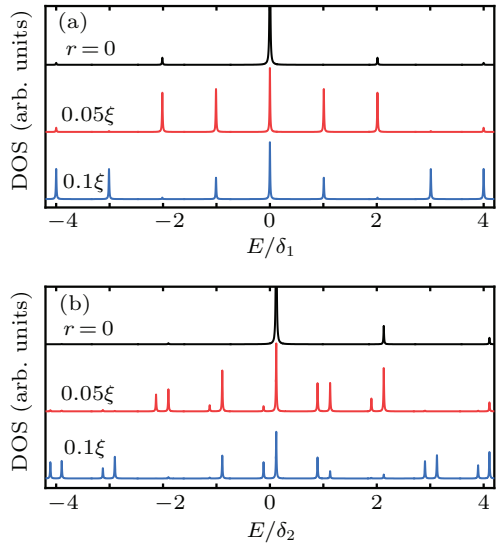


Fig. 2. The calculated DOS near vortex cores along the $\theta = 45°$ direction for the above two band structures shown in Fig. 1. The energy of the horizontal axis is normalized by δ_1 (δ_2), with the average level spacing of about $0.00147t_1$ ($0.00151t_1$).

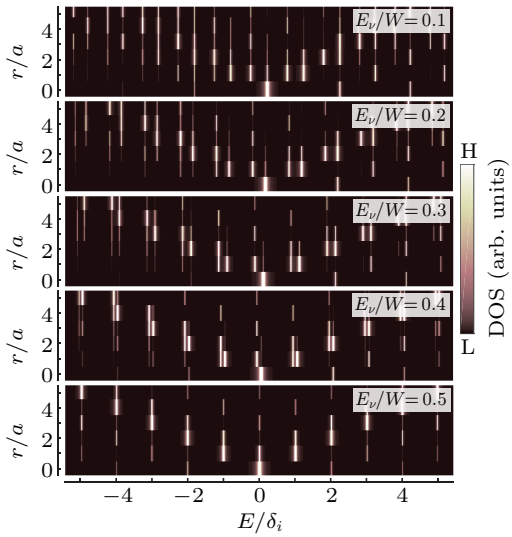


Fig. 3. The spatial evolutions of the DOS along the $\theta = 0°$ direction for five different band structures with VHSs and Fermi levels located at $0.1W$, $0.2W$, $0.3W$, $0.4W$, and $0.5W$ from the band bottom. For each figure, the energy of the horizontal axis is normalized by the average level spacing δ_i (in the range from $0.00147t_1$ to $0.00167t_1$, explicit values can be found in the supplementary materials).

The similar splitting behavior can also be acquired when the Fermi level moves slightly away from the VHS which is fixed at the middle of the band. When the Fermi level and VHS are both at the band middle, there is exactly one electron per site ($\mu = 0$). If the band filling n is smaller than 1, the Fermi level will move away from the VHS to the band bottom. Figure 4 shows the spatial evolutions of the DOS along the $\theta = 0°$ direction for the same band ($E_v/W = 0.5$) but with different fillings n. For each figure, the energy of the horizontal axis is normalized by the average level spacing δ_i. One can see the similar features including the peak-splitting behavior from Fig. 4. When the Fermi level is about $0.0274t_1$ away from the VHS ($n = 0.980$), discrete vortex bound states are close to the half-odd-integer quantization. It should be pointed out that even for the $n = 0.980$ case the VHS is still inside the $0.05t_1$ gap.

From the above two spectral evolutions (Figs. 3 and 4), it can be found that the particle–hole symmetric point of the electronic band may be responsible for the emergence of integer quantized vortex core states. Because the dispersion relation with a VHS near the Fermi level is tricky to be handled within a traditional analytical calculation, few related works have considered this situation. On the other hand, the experimental detection of the integer quantized vortex bound states has been realized in a variety of iron-based superconductors,[4–7,9] which were referred to as signals of Majorana zero modes. Our theoretical calculation based on large-scale lattice model gives an alternative explanation of integer quantized states. For the complexity of the multi-band electronic structure, it is possible for the emergence of a VHS near the Fermi level in certain doping range. If the corresponding electronic band is highly particle-hole symmetric at the same time, the band origin of zero modes should be considered.

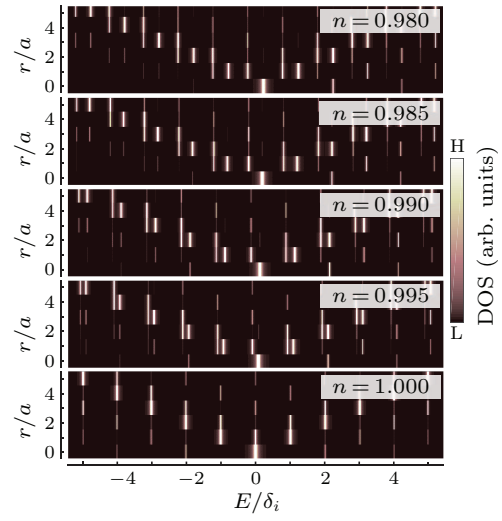


Fig. 4. The spatial evolutions of the DOS for the same band ($E_v/W = 0.5$) but with different fillings n. The case of the Fermi level lying exactly at the VHS corresponds to the band filling $n = 1$. For each figure, the spectra at vortex core and five nearest sites along the $\theta = 0°$ direction are shown, and the energy of the horizontal axis is normalized by the average level spacing δ_i (in the range from $0.00147t_1$ to $0.00149t_1$, explicit values can be found in the supplementary materials).

4. Conclusion

In summary, we have performed a BdG calculation to study the discrete vortex bound states by considering several one-band structures with VHSs in the vicinity of the Fermi level. Our calculation shows that the VHS near the Fermi level can dramatically change the arrangement of quantized vortex bound states. When the VHS and Fermi level are both exactly at the band middle, a zero-energy bound state will emerge around the vortex core. Energy ratios of other higher-energy states follow integer numbers. These vortex bound state peaks have a splitting behavior when the VHS together with the Fermi level moves away from the middle of the band or when the Fermi level moves slightly away from the VHS which is fixed at the band middle. The splitting behavior will eventually lead to a rearrangement of conventional CdGM states whose energy ratios follow half-odd-integer numbers.

Acknowledgements

Project supported by the National Natural Science Foundation of China (Grant No. 11804154), and the Scientific Research Foundation of NJIT (Grant Nos. YKJ201853 and CKJA201807).

References

[1] Caroli C, de Gennes P G and Matricon J 1964 *Phys. Lett.* **9** 307
[2] Hayashi N, Isoshima T, Ichioka M and Machida K 1998 *Phys. Rev. Lett.* **80** 2921
[3] Chen M Y, Chen X Y, Yang H, Du Z Y, Zhu X Y, Wang E Y and Wen H H 2018 *Nat. Commun.* **9** 970
[4] Kong L Y, Zhu S Y, Papaj M, Chen H, Cao L, Isobe H, Xing Y Q, Liu W Y, Wang D F, Fan P, Sun Y J, Du S X, Schneeloch J, Zhong R D, Gu G D, Fu L, Gao H J and Ding H 2019 *Nat. Phys.* **15** 1181
[5] Machida T, Sun Y, Pyon S, Takeda S, Kohsaka Y, Hanaguri T, Sasagawa T and Tamegai T 2019 *Nat. Mater.* **18** 811
[6] Liu Q, Chen C, Zhang T, Peng R, Yan Y J, Wen C H P, Lou X, Huang Y L, Tian J P, Dong X L, Wang G W, Bao W C, Wang Q H, Yin Z P, Zhao Z X and Feng D L 2018 *Phys. Rev. X* **8** 041056
[7] Chen C, Liu Q, Zhang T Z, Li D, Shen P P, Dong X L, Zhao Z X, Zhang T and Feng D L 2019 *Chin. Phys. Lett.* **36** 057403
[8] Chen C, Liu Q, Bao W C, Yan Y J, Wang Q H, Zhang T and Feng D L 2020 *Phys. Rev. Lett.* **124** 097001
[9] Liu W Y, Cao L, Zhu S Y, Kong L Y, Wang G W, Papaj M, Zhang P, Liu Y B, Chen H, Li G, Yang F Z, Kondo T, Du S X, Cao G H, Shin S, Fu L, Yin Z P, Gao H J and Ding H 2020 *Nat. Commun.* **11** 5688
[10] Chen X Y, Duan W, Fan X W, Hong W S, Chen K L, Yang H, Li S L, Luo H Q and Wen H H 2021 *Phys. Rev. Lett.* **126** 257002
[11] Fan X W, Chen X Y, Yang H and Wen H H 2021 *Europhys. Lett.* **136** 46002
[12] Kim H, Nagai Y, Rózsa L, Schreyer D and Wiesendanger R 2021 *Appl. Phys. Rev.* **8** 031417
[13] Wang Y, Hirschfeld P J and Vekhter I 2012 *Phys. Rev. B* **85** 020506
[14] Fang D L 2022 *Chin. Phys. B* to be published
[15] van Hove L 1953 *Phys. Rev.* **89** 1189
[16] Furukawa N, Rice T M and Salmhofer M 1998 *Phys. Rev. Lett.* **81** 3195
[17] Nandkishore R, Levitov L S and Chubukov A V 2012 *Nat. Phys.* **8** 158
[18] Yao H and Yang F 2015 *Phys. Rev. B* **92** 035132
[19] Meng Z Y, Yang F, Chen K S, Yao H and Kee H Y 2015 *Phys. Rev. B* **91** 184509
[20] Sherkunov Y and Betouras J J 2018 *Phys. Rev. B* **98** 205151
[21] Hu Y, Wu X X, Ortiz B R, Ju S L, Han X L, Ma J Z, Plumb N C, Radovic M, Thomale R, Wilson S D, Schnyder A P and Shi M 2022 *Nat. Commun.* **13** 2220
[22] Li G H, Luican A, Lopes Dos Santos J M B, Castro Neto A H, Reina A, Kong J and Andrei E Y 2009 *Nat. Phys.* **6** 109
[23] Fang D L, Shi X, Du Z Y, Richard P, Yang H, Wu X X, Zhang P, Qian T, Ding X X, Wang Z Y, Kim T K, Hoesch M, Wang A F, Chen X H, Hu J P, Ding H and Wen H H 2015 *Phys. Rev. B* **92** 144513
[24] Kang M G, Fang S A, Kim J K, Ortiz B R, Ryu S H, Kim J, Yoo J, Sangiovanni G, Di Sante D, Park B G, Jozwiak C, Bostwick A, Rotenberg E, Kaxiras E, Wilson S D, Park J H and Comin R 2022 *Nat. Phys.* **18** 301
[25] Udby L, Andersen B M and Hedegård P 2006 *Phys. Rev. B* **73** 224510
[26] Wang D, Xu J, Xiang Y Y and Wang Q H 2010 *Phys. Rev. B* **82** 184519
[27] Fang D L, Liu J S and Cui Y K 2021 *Phys. C* **591** 1353963